

(H₁₁O₅)⁺ pentamer system illustrated in Figure 6b. The two additional waters were placed as shown at a distance of 2.54 Å from the oxygen atoms of the neighboring waters, and the geometry of the remainder of the system was left unaltered from that shown in Figure 6a. Once again, the energy was calculated as a function of the positions of the two central protons H_a and H_b while all other nuclei were held stationary. The isoenergy contours for the pentamer, shown in Figure 6b, exhibit many of the same qualitative features as the potential energy surface for the trimer. For example, the transition states for both systems occur when one proton has been partially transferred and the other remains on the central water. The transition state for the pentamer is found to occur slightly later ($r_a = 1.5$ Å) than for the trimer (1.6 Å). Other quantitative changes include an increase in the activation energy from 10 to 16 kcal/mol on going from the trimer to the pentamer. Also, the (H₂O)(H₃O)⁺(H₂O) configuration is only 2 kcal/mol more stable than (H₃O)⁺(H₂O)(H₂O) in the pentamer whereas the analogous quantity was 14 kcal/mol in the trimer.

All of the above changes may in fact be attributed to the attenuation of end effects in the pentamer as compared to the trimer. As mentioned previously, association of a third proton with a terminal water represents a rather unfavorable situation for the trimer as only one hydrogen bond is available to help alleviate the charge. In the pentamer, however, the same molecule is involved in two hydrogen bonds as is the central water. Consequently, the configuration in which the charge is associated with the central water is approximately equal in energy to that in which

the extra proton is on an adjacent molecule. This near equality indicates that end effects have been greatly reduced and that the pentamer presents us with a realistic picture of the situation in long hydrogen bond chains. The activation energy of 16 kcal/mol found for the pentamer is approximately the same as that calculated for the dimer and tetramer with the same value of R (see Figure 1). This fact again points to the reliability of calculations involving only the dimer in obtaining activation energies for proton transfers in larger systems. Comparisons of the potential surfaces of H⁺(H₂O)_{*n*}, $n = 2, 3, 4,$ and 5 for $R = 2.75$ and $R = 2.55$, all lead to the same conclusions as drawn here for $R = 2.95$.

The transition state in the pentamer involves the partial transfer of only one proton. From the transition-state configuration, the energy of the system decreases monotonically toward either the single- or double-proton transferred products. It therefore appears that once enough energy has been harnessed to achieve the transition state which involves partial transfer of one proton, the transfer of a second proton may be coupled to the completion of the transfer with no additional expense in energy. This fact is suggestive that perhaps in the longer hydrogen bond chains, a large number of protons may be transferred simultaneously at no more cost in energy than only a single transfer.

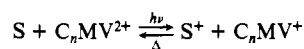
Acknowledgment. I wish to thank Professor John F. Nagle for making available results prior to publication and the Southern Illinois University Academic Computing Center for a grant of computer time. This work was supported in part by the Research Corp.

Photoredox Reactions in Functional Micellar Assemblies. Use of Amphiphilic Redox Relays To Achieve Light Energy Conversion and Charge Separation

Pierre-Alain Brugger, Pierre P. Infelta, André M. Braun, and Michael Grätzel*

Contribution from the Institut de Chimie Physique, Ecole Polytechnique Fédérale, 1015 Lausanne, Switzerland. Received April 7, 1980

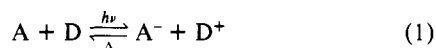
Abstract: The photoreduction of a homologous series of amphiphilic viologens (C_{*n*}MV²⁺) using Ru(bpy)₃²⁺ and zinc tetraakis(*N*-methylpyridyl)porphyrin (ZnTMPyP⁴⁺) as sensitizers (S) was studied in water and aqueous solution containing cationic micelles.



Here, C_{*n*}MV²⁺ stands for *N*-alkyl-*N*'-methyl-4,4'-dipyridinium dichloride (alkyl = dodecyl (C₁₂MV²⁺), tetradecyl (C₁₄MV²⁺), hexadecyl (C₁₆MV²⁺), and octadecyl (C₁₈MV²⁺)). The forward electron transfer occurs with the viologen present in the aqueous phase. Upon reduction the relay acquires hydrophobic properties leading to rapid solubilization in the micelles. The subsequent thermal back-reaction is impaired by the positive surface potential of the aggregates. This decreases the rate constant for the electron back-transfer at least 500-fold. The stabilization and yield of redox products are optimal in a system containing ZnTMPyP⁴⁺ as the sensitizer, C₁₄MV²⁺ as a relay, and cetyltrimethylammonium chloride micelles. A kinetic model is presented to explain the effects observed, and implications for energy conversion systems are discussed.

Introduction

In the photoredox reaction



light acts as an electron pump¹ promoting charge transfer from

the donor (D) to the acceptor (A) under production of the high energy intermediates A⁻ and D⁺. If the chemical potential of A⁻ and D⁺ is to be utilized in subsequent fuel-generating processes, it is mandatory to prevent or retard the energy wasting back-reaction.² Molecular organizations such as micelles can serve this purpose since they possess charged microscopic interfaces which afford an electrostatic barrier to accomplish the charge

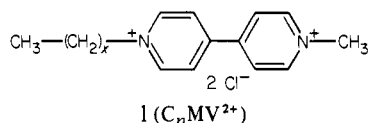
(1) Balzani, V.; Moggi, L.; Manfrin, M. F.; Bolletta, F.; Gleria, M. *Science (Washington D.C.)* **1975**, *189*, 852. (b) Calvin, M. *Photochem. Photobiol.* **1976**, *23*, 425. Porter, G.; Archer, M. D. *ISR, Interdiscip. Sci. Rev.* **1976**, *1*, 119. (d) Bolton, J. R., Ed. "Solar Power and Fuels"; Academic Press: New York, 1977. (e) Bolton, J. R. *Science (Washington, D.C.)* **1978**, *202*, 105. (f) Pioneering work on photoredox reactions in homogeneous systems was carried out by Weller et al.; see, for example: Knibbe, H.; Rehm, D.; Weller, A. *Ber. Bunsenges. Phys. Chem.* **1969**, *73*, 839; Rehm, D.; Weller, A. *Ibid.* **1969**, *73*, 834. (g) For a recent review see also: Schumacher, E. *Chimica* **1978**, *32*, 193.

(2) For kinetic control of light-induced redox reaction by using: (a) BLM, cf.: Tien, H. T. *Top. Photosynth.* **1979**, *3*, 116-173. (b) Monolayers, cf.: Kuhn, H. J. *Photochem.* **1979**, *10*, 111. (c) Vesicles, cf.: Ford, W. E.; Otvos, J. W.; Calvin, M. *Proc. Natl. Acad. Sci. U.S.A.* **1979**, *76*, 3590. Ford, W. E.; Otvos, J. W.; Calvin, M. *Nature (London)* **1978**, *274*, 507. Calvin, M. *Int. J. Energy Res.* **1979**, *3*, 73. Infelta, P. P.; Fendler, J. H.; Grätzel, M. *J. Am. Chem. Soc.* **1980**, *102*, 1479.

separation process.³ Functional assemblies in which part of the micelle-forming surfactant participates in the redox events have exhibited promising cooperative effects.⁴

In this paper we shall illustrate the favorable intervention of amphiphilic electron relays in a photoredox reaction which is of great importance for the design of a cyclic water decomposition system.

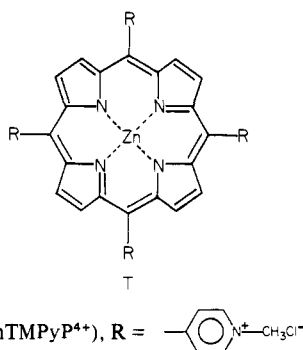
The process to be considered is the reduction of a functional viologen



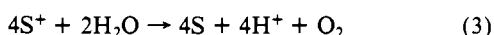
where $x = 11, 13, 15,$ and 17 , by the excited state of a sensitizer (S)



As a sensitizer we selected the tris(bipyridine) complex of ruthenium ($Ru(bpy)_3^{2+}$) and the water-soluble porphyrin, zinc tetrakis(*N*-methylpyridyl)porphyrin



Both species have the appropriate redox potential to afford water oxidation via⁵



The reduced-electron relay, on the other hand, is capable of generating hydrogen from water⁶



The sequence of reactions 1–3 constitutes cyclic water cleavage

(3) (a) Grätzel, M. In "Micellization and Microemulsions"; Mitall, K. L., Ed.; Plenum Press: New York, 1977; Vol 2, p 591. (b) Grätzel, M. *Isr. J. Chem.* **1979**, *18*, 3. (c) Wolff, C.; Grätzel, M. *Chem. Phys. Lett.* **1977**, *52*, 542. (d) Waka, Y.; Hamamoto, K.; Mataga, N. *Ibid.* **1978**, *53*, 242. (e) Razem, B.; Wong, M.; Thomas, J. K. *J. Am. Chem. Soc.* **1978**, *100*, 1629. (f) Alkaiatis, S. A.; Beck, G.; Grätzel, M. *Ibid.* **1975**, *97*, 5723. (g) Alkaiatis, S. A.; Grätzel, M. *Ibid.* **1976**, *98*, 3549. (h) Maestri, M.; Infelta, P. P.; Grätzel, M. *J. Chem. Phys.* **1978**, *69*, 1522.

(4) (a) Moroi, Y.; Braun, A. M.; Grätzel, M. *J. Am. Chem. Soc.* **1979**, *101*, 567. (b) Moroi, Y.; Infelta, P. P.; Grätzel, M. *Ibid.* **1979**, *101*, 573. (c) Humphry-Baker, R.; Grätzel, M.; Tundo, P.; Pelizzetti, E. *Angew. Chem., Int. Ed. Engl.* **1979**, *18*, 630. (d) Pileni, M. P.; Braun, A. M.; Grätzel, M. *Photochem. Photobiol.* **1980**, *31*, 423.

(5) Reaction 3 proceeds in the presence of a suitable redox catalyst, cf.: (a) Kiwi, J.; Grätzel, M. *Angew. Chem., Int. Ed. Engl.* **1978**, *17*, 860; (b) Kiwi, J.; Grätzel, M. *Chimia* **1979**, *33*, 289; (c) Grätzel, M. In "Dahlem Conferences 1978 on Light-Induced Charge Separation"; Gerischer, H., Katz, J. J., Eds.; Verlag Chemie: Weinheim/Bergstr.: West Germany, 1979; p 299; (d) Kiwi, J.; Grätzel, M. *Angew. Chem., Int. Ed. Engl.* **1979**, *18*, 624; (e) Kalayanasundaram, K.; Micic, O.; Pramauro, E.; Grätzel, M. *Helv. Chim. Acta* **1979**, *62*, 2432; (f) Kiwi, J. *Isr. J. Chem.* **1979**, *18*, 369; (g) Lehn, J. M.; Sauvage, J. P.; Ziessel, R. *Nouv. J. Chim.* **1979**, *3*, 423; (h) Shafirovich, V. Ya.; Khannanov, N. K.; Strelets, V. V. *Ibid.* **1980**, *4*, 81. The potential of the S/S^+ couples are sufficiently positive to afford oxygen evolution; i.e., $E^0(Ru(bpy)_3^{3+/2+}) = 1.26$ V (cf.: Creutz, C.; Sutin, N. *Proc. Natl. Acad. Sci. U.S.A.* **1975**, *72*, 2858) and $E^0(TMPyP^{5+/4+}) = 1.2$ V (cf.: Kalayanasundaram, K.; Neumann-Spallart, M., in press).

(6) The redox potential of simple methyl viologen is -0.45 V (cf.: Michaelis, L.; Hill, E. S. *J. Gen. Physiol.* **1933**, *16*, 859; Elotson, R. M.; Edsberg, R. L. *Can. J. Chem.* **1957**, *35*, 646; Hornbaugh, J. E.; Sandquist, J. E.; Burris, R. H.; Orme-Johnson, W. H. *Biochemistry* **1976**, *15*, 2633); introduction of long alkyl chains does not change the E^0 value significantly (cf.: Van Dam, H. T.; Ponjee, J. J. *J. Electrochem. Soc.* **1974**, *121*, 1555).

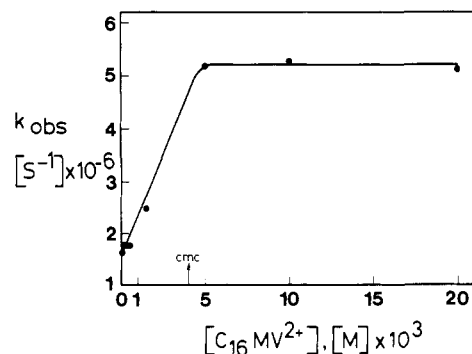
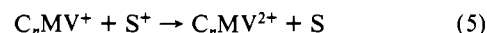


Figure 1. Effect of $C_{16}MV^{2+}$ concentration on the observed rate constant of the decay of the $Ru(bpy)_3^{2+}$ (CT) emission ($[Ru(bpy)_3^{2+}] = 10^{-4}$ M). Time-resolved luminescence at 620 nm was measured by laser technique.

by light which can be effected either in a combined catalytic⁷ or in a separated half-cell system.⁸ In both cases, it is desirable to prevent or at least retard the back-reaction



A micellar system which achieves this goal is now described in detail.⁹

Experimental

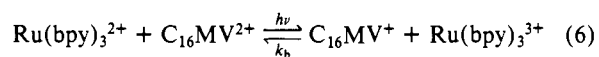
Materials. The surfactant analogues of *N*-methyl-4,4'-bipyridinium chloride were synthesized according to a procedure published elsewhere.¹⁰ $Ru(bpy)_3^{2+}Cl_2$ (Strem) was used as supplied. $ZnTMPyP^{4+}$ was prepared from the free porphyrin as outlined earlier.²⁵ Cetyltrimethylammonium chloride (CTAC), Eastman Kodak, was purified by threefold recrystallization from an acetone–water mixture (90/10; v/v). Octadecyltrimethylammonium chloride (>99.5%) was generously supplied by Hoechst AG, West Germany. Dodecyltrimethylammonium chloride (DTAC), Eastman Kodak, was treated by Soxhlet extraction with hexane and subsequently recrystallized from water. Cetylpyridinium chloride (Fluka purum) was purified by dissolving in an acetone–water mixture (90%; v/v) and subsequent precipitation by addition of ether. This procedure was repeated at least six times. Deionized water was distilled from alkaline permanganate and subsequently twice from a quartz still. All other chemicals were at least reagent grade and used as supplied by the vendor.

Apparatus. Laser photolysis experiments were performed with a JK-2000 frequency doubled (530 nm) neodymium laser with a pulse width of 12 ns. The photomultiplier system used for kinetic spectroscopy has already been previously described.¹¹ The detection of transient absorbance changes in the 650–1050 nm region was performed by using an E66-SHS-100 diode with a rise time less than 4 ns when being operated at 125 V. The time course of the optical events was recorded with a Tektronix WP-221 data acquisition system equipped with two R-7912 transient digitizers, which allows for simultaneous recording on two different time scales.

For continuous illumination we used a 1000-W halogen lamp in connection with an infrared filter. For comparative studies, eight samples each containing 5 mL of solution were irradiated simultaneously. The cells were thermostated at 25 °C. Hydrogen was analyzed by means of a Gow-Mac thermal conductivity detector with a limit of 1 nmol. A Carbosieve 5A column was used at 35 °C.

Results and Discussion

(a) Effects of Micelle Formation on the Light-Induced Reduction of $C_{16}MV^{2+}$ by $Ru(bpy)_3^{2+}$. In this section we shall explore the kinetics of reduction of $C_{16}MV^{2+}$ by the excited state of $Ru(bpy)_3^{2+}$.



(7) Kalayanasundaram, K.; Grätzel, M. *Angew. Chem., Int. Ed. Engl.* **1979**, *18*, 701.

(8) Neumann-Spallart, M.; Kalayanasundaram, K.; Grätzel, C. K.; Grätzel, M. *Helv. Chim. Acta* **1980**, *63*, 1111.

(9) A preliminary report has appeared, cf.: Brugger, P. A.; Grätzel, M. *J. Am. Chem. Soc.* **1980**, *102*, 2461.

(10) Krieg, M.; Braun, A. M.; Pileni, M. P.; Grätzel, M. *J. Colloid Interface Sci.*, in press. For a list of CMC values compare Table I.

(11) Rothenberger, G.; Infelta, P. P.; Grätzel, M. *J. Phys. Chem.* **1979**, *83*, 1871.

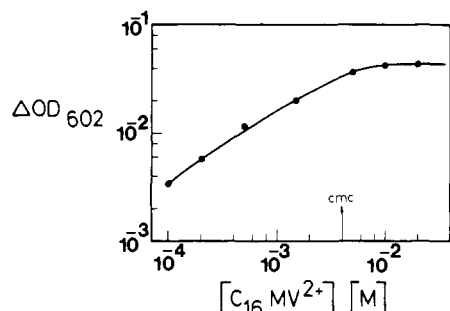


Figure 2. Effect of $C_{16}MV^{2+}$ concentration on the yield of reduced viologen obtained from the oxidative quenching of $Ru(bpy)_3^{2+}$ excited states. Data obtained from the laser photolysis of 10^{-4} M $Ru(bipy)_3^{2+}$ solutions. ΔOD_{602} represents the optical density change at 602 nm produced by light excitation and measured after completion of the forward electron transfer.

In particular, the question will be addressed whether the amphiphilic electron relay exhibits a different reactivity in the micellized as compared to the monomer state. The Ru complex was excited by the 530-nm laser pulse and the decay of the excited state monitored by its characteristic emission at 620 nm or its absorption at 365 nm.¹² The specific rate of deactivation is plotted as a function of $C_{16}MV^{2+}$ concentration in Figure 1. In viologen-free solution the decay constant is 1.62×10^8 s⁻¹, which agrees with literature values. The specific rate increases linearly with $C_{16}MV^{2+}$ concentration until at ca. 4×10^{-3} M a plateau is attained from whereon no further augmentation is observed. It is important to note that the breakpoint in the curve coincides with the CMC of $C_{16}MV^{2+}$. From this behavior, one infers that the contribution of micellized $C_{16}MV^{2+}$ to the deactivation of $Ru(bpy)_3^{2+}$ excited states is negligible, the electron transfer occurring exclusively with the monomer form of the acceptor present in the aqueous bulk phase. Such a behavior is rationalized in terms of the highly repulsive positive surface potential of the $C_{16}MV^{2+}$ micelles that impairs any approach of the cationic sensitizer. From the slope of the straight line in Figure 1 observed in the low concentration range, one obtains¹³ $k_q = 6.7 \times 10^8$ M⁻¹ s⁻¹. Consistent with this interpretation is the effect of $C_{16}MV^{2+}$ concentration on the yield of redox products obtained from reaction 6 (Figure 2). This can be determined from the transient optical density at 602 nm where $C_{16}MV^{2+}$ possesses a characteristic absorption maximum.¹⁴ ΔOD_{602} increases with $C_{16}MV^{2+}$ concentration until it reaches a plateau at the CMC point. The absorption confirms that $C_{16}MV^{2+}$ in the micellar form is unable to interact with the $Ru(bpy)_3^{2+}$ excited states.

In order to characterize a photoredox reaction, it is of interest to evaluate the efficiency of the electron-transfer quenching η_{re} . This parameter defines the fraction of redox products that escape from solvent cage recombination. For simple methylviologen $\eta_{re} = 0.3$.¹⁵ As the $Ru(bpy)_3^{2+}$ excited state is formed with unit quantum efficiency, this number gives also the limiting quantum yield of methyl viologen reduction at infinite quencher concentration. The concentration of $C_{16}MV^{2+}$ produced by the laser flash was calculated from ΔOD_{602} by using Beer's law and an extinction coefficient¹⁶ of 11500 M⁻¹ cm⁻¹. Figure 3 shows a plot of $1/[C_{16}MV^+]$

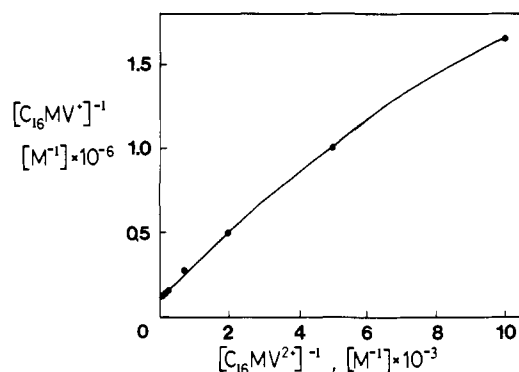


Figure 3. Effect of $C_{16}MV^{2+}$ concentration of the yield of $C_{16}MV^+$ obtained from oxidation quenching of the $Ru(bpy)_3^{2+}$ excited states. Data from Figure 2 are replotted according to eq 7.

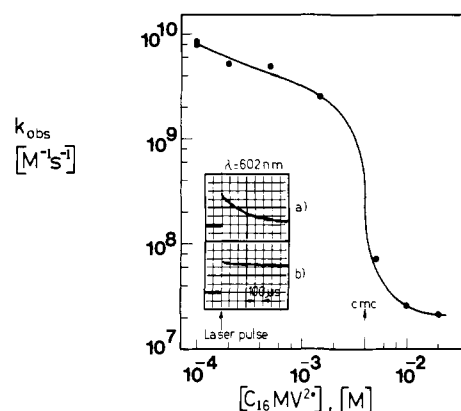


Figure 4. Effect of $C_{16}MV^{2+}$ concentration on the observed rate constant of the electron back-transfer between $C_{16}MV^+$ and $Ru(bpy)_3^{3+}$ ($[Ru(bpy)_3^{2+}] = 10^{-4}$ M). The insert shows representative oscillograms showing the temporal behavior of the $C_{16}MV^+$ absorption at 602 nm: (a) $[C_{16}MV^{2+}] = 5 \times 10^{-4}$ M; (b) $[C_{16}MV^{2+}] = 2 \times 10^{-2}$ M.

$[C_{16}MV^+]$ against the reciprocal $C_{16}MV^{2+}$ concentration. From simple solution kinetics one would expect a linear relation

$$\frac{1}{[C_{16}MV^+]} = \frac{1}{{}^0Ru(bpy)_3^{2+}(CT)\eta_{re}} + \frac{1}{{}^0Ru(bpy)_3^{2+}(CT)\eta_{re}} \frac{k_0}{k_q} \frac{1}{[C_{16}MV^{2+}]} \quad (7)$$

Here, ${}^0Ru(bpy)_3^{2+}(CT)$ designates the initial excited-state concentration produced by the flash while k_0 is the specific rate of deactivation in the absence of quencher. The initial concentration of excited states was calculated from the optical density change at 365 nm by using the extinction coefficient of $Ru(bpy)_3^{2+}(CT)$ determined earlier.¹⁷ From the ordinate intercept in Figure 3, one derives then $\eta_{re} = 30\%$, which corresponds to the yield obtained for simple methyl viologen. The ratio of the slope to intercept in the linear region of Figure 3 gives $k_0/k_q = 2.1 \times 10^{-3}$ M. From Figure 1 we obtained $k_q = 6.7 \times 10^8$ M⁻¹ s⁻¹ and $k_0/k_q = 2.4 \times 10^{-3}$ M. Both values are in satisfactory agreement.

Having assessed the micellar effects of the forward electron-transfer process, we shall now turn our attention to the thermal back-reaction involving $C_{16}MV^+$ and $Ru(bpy)_3^{3+}$. The kinetic analysis was performed by monitoring the absorption of the former species at 602 nm and the bleaching recovery of $Ru(bpy)_3^{2+}$ at 470 nm.¹⁸ Results are displayed in Figure 4. The upper inserted

(12) (a) Bensasson, R.; Salet, C.; Balzani, V. *J. Am. Chem. Soc.* **1976**, *98*, 3722. (b) Sutin, N.; Creutz, C. *Adv. Chem. Ser.* **1978**, No. 168. (c) Bensasson, R.; Salet, C.; Balzani, V. *C. R. Hebd. Seances Acad. Sci., Ser. B* **1979**, *T289*, 41. (d) Lachish, U.; Infelta, P. P.; Grätzel, M. *Chem. Phys. Lett.* **1979**, *62*, 317. (e) Creutz, C.; Chou, M.; Netzel, T. L.; Okumura, M.; Sutin, N. *J. Am. Chem. Soc.* **1980**, *102*, 1309. It is now agreed upon (cf. ref 10d,e) that the extinction coefficient of the $Ru(bpy)_3^{2+}$ charge-transfer excited state at 360 nm is ca. 25000 M⁻¹ cm⁻¹. Earlier reports (ref 10b,c) gave too low extinction coefficients.

(13) The kinetic salt effect induces a slight acceleration of the reaction with increasing surfactant concentration. A detailed discussion of ionic strength effects on the reduction of MV^{2+} by $Ru(bpy)_3^{2+}$ excited states is given by: Gaines, G. L. *J. Phys. Chem.* **1979**, *83*, 3088.

(14) Trudinger, P. A. *Anal. Biochem.* **1970**, *36*, 222.

(15) Kalyanasundaram, K.; Kiwi, J.; Grätzel, M. *Helv. Chim. Acta* **1978**, *61*, 2720.

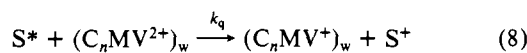
(16) Steckhan, E.; Kuwana, T. *Ber. Bunsenges. Phys. Chem.* **1974**, *78*, 253.

(17) Cf. ref 12d.

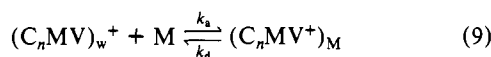
(18) Without exception, the kinetics of the bleaching recovery at 470 nm always presented the exact mirror image of the 602-nm decay. Hence, stabilization of the reduced viologen always implies stabilization of the oxidized sensitizer.

oscillogram shows the time evolution of the optical density at 602 nm in dilute solutions of $C_{16}MV^{2+}$ where no micelles are present. The transient absorption produced after the laser pulse decays here rapidly within a time domain of several hundred microseconds. In striking contrast to this behavior stand the kinetics observed in the presence of $C_{16}MV^{2+}$ micelles. The lower oscillogram illustrates that the 602-nm absorbance is here practically stable over 1 ms. An exact mirror image of this step function is observed for the bleaching of the 470-nm absorption of $Ru(bpy)_3^{2+}$. Apparently, the micellar aggregates enhance significantly the lifetime of the redox products from reaction 6. In order to quantitatively assess the micellar inhibition of the back-reaction, we determined the second-order rate constant k_{obsd} as a function of $C_{16}MV^{2+}$ concentration. Below the CMC k_{obsd} assumes values which are close to the diffusion-controlled limit. It decreases slightly with $C_{16}MV^{2+}$ concentration. This effect is accelerated drastically in the vicinity of the CMC where k_{obsd} drops by several orders of magnitude. In fact, the k_{obsd} values obtained above the CMC can only be considered as upper limits, as the controlling factor for the $C_{16}MV^+$ lifetime becomes the reaction with impurities, notably O_2 .

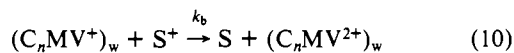
(b) Kinetic Interpretation. It was shown above that the photoredox reaction between the sensitizer and the electron relay takes place exclusively in the aqueous phase.



Here, the subscript w refers to species that are present in water and not associated with the micelles. Upon reduction the surfactant viologen undergoes a pronounced increase in hydrophobicity. As a consequence, the reduced form shows a strong tendency to associate with surfactant micelles



Under our experimental condition at most one C_nMV^+ is associated with one micelle. Reaction 9 is reversible as the dissociation of the reduced relay from the micelle has to be taken into account. As for the electron back-transfer, it may safely be assumed that this also can only occur in the aqueous phase.



The oxidized sensitizer is prevented from approaching the cationic micelles by their repulsive surface charge. As the ζ potential of the type of aggregates employed in this study is about +100 mV¹⁹ the probability of encounter²⁰ with $Ru(bpy)_3^{3+}$ and $(ZnTMPyP)^{5+}$ is only $\sim 6 \times 10^{-6}$ and $\sim 2 \times 10^{-9}$, respectively.

From eq 9 and 10, we find the following differential time laws:

$$d[S^+]/dt = -k_b[S^+][(C_nMV^+)_w] \quad (11)$$

$$d[(C_nMV^+)_w]/dt = -k_b[S^+][(C_nMV^+)_w] - k_a[M][(C_nMV^+)_w] + k_d[(C_nMV^+)_M] \quad (12)$$

$$d[(C_nMV^+)_M]/dt = k_a[M][(C_nMV^+)_w] - k_d[(C_nMV^+)_M] \quad (13)$$

Equilibrium 9 is established with a relaxation time of $\tau_R = 1/(k_a[M] + k_d)$. The specific rate of association may be estimated²² as $\sim 10^9 M^{-1} s^{-1}$. As the concentration of micelles employed exceeds always $10^{-4} M$, the upper limit for τ_R is $10^{-5} s$. It may therefore be assumed that equilibrium conditions are applicable

for almost the whole part of the back-reaction. This provides the additional relation (14), where we have taken into account that

$$[(C_nMV^+)_w] \simeq [S^+]/(1 + (k_a/k_d)[M]) \quad (14)$$

the concentration of oxidized sensitizer and reduced relay is equal. Inserting eq 14 into (11), one finds finally for the long-time domain eq 15 which corresponds to a second-order rate law, (16), with

$$d[S^+]/dt \simeq -k_b/(1 + (k_a/k_d)[M])[S^+]^2 \quad (15)$$

$$k_{obsd} = k_b/(1 + k_a[M]/k_d) \quad (16)$$

the observed rate constant. Another approximate solution of the differential equations includes the consideration of the short-time domain where the equilibrium 9 is not yet established. Here, we part from eq 12 and 13 and neglect the quadratic term in the first relation.²¹ This allows integration and yields the ratio

$$\frac{[(C_nMV^+)_M]}{[(C_nMV^+)_w]} = \frac{k_a[M](1 - \exp[-(k_a[M] + k_d)t])}{k_d + k_a[M] \exp[-(k_a[M] + k_d)t]} \quad (17)$$

Equation 17 reduces to the mass action law for equilibrium 9 at longer times. It is used together with the relation $[S^+] = [(C_nMV^+)_w] + [(C_nMV^+)_M]$ in eq 11 to yield the integrated rate law (18). It should be noted that eq 18 in the long-time limit

$$\frac{1}{[S^+]} \simeq \frac{1}{[S^+]_{t=0}} + \frac{k_b t}{1 + k_a[M]/k_d} + \frac{k_a k_b [M]}{(k_a[M] + k_d)^2} (1 - e^{-(k_a[M] + k_d)t}) \quad (18)$$

gives also a second-order law. The micellar inhibition of the back-reaction between oxidized sensitizer and reduced relay is expressed quantitatively by the ratio k_{obsd}/k_b , eq 16. The dissociation rate k_d for a hydrophobic entity such as C_nMV^+ is likely to be smaller than $10^3 s^{-1}$.²² If the surfactant aggregates are present in $10^{-4} M$ concentration, one obtains $k_{obsd}/k_b < 10^{-2}$ corresponding to at least 100-fold reduction in the back-reaction rate.

(c) Charge Separation with Simple Detergent Micelles. The kinetic model outlined above was based on the concept that the hydrophilic electron relay upon reduction acquires a pronounced hydrophobic character. This leads to rapid solubilization in the cationic surfactant assembly and inhibition of the back-reaction. Such an effect should not be restricted to the case of $C_{16}MV^{2+}$ micelles treated in paragraph a. Rather, it should be accomplished by any aggregate providing hydrophobic sites for the solubilization of the reduced electron relay and a positive surface charge for the repulsion of the sensitizer cation.

This idea is borne out by results obtained with a variety of micellar assemblies formed by detergents such as DTAC, CTAC, cetylpyridinium chloride and octadecyltrimethylammonium chloride as well as cationic surfactant vesicles. Consider for example the effect of CTAC on the light-induced reduction of $C_{14}MV^{2+}$ by the excited state of $Ru(bpy)_3^{3+}$. In the absence of CTAC, the forward electron transfer occurs with a specific rate²³ of $7 \times 10^8 M^{-1} s^{-1}$ while the back-reaction has a rate constant of $4 \times 10^9 M^{-1} s^{-1}$. Analysis of the $C_{14}MV^+$ decay in micelle-free solution reveals that deviations from a second-order behavior occur in the long-time domain, i.e., after ca. 2 half-lifetimes. The return to the zero level occurs here faster than expected from a simple

(21) This assumption is reasonable, at least for not too low a micellar concentration, as the equilibrium relaxation will occur faster than the back-reaction.

(22) The exit rate of a surfactant molecule from a micelle decreases drastically with increasing chain length. Thus, k_d is $1.3 \times 10^9 s^{-1}$ for hexyl sulfate while it is only $6 \times 10^4 s^{-1}$ for hexadecyl sulfate. In contrast, the chain length exerts only a minor influence on the entry rate constant for which values $> 10^9 M^{-1} s^{-1}$ are common, cf.: Aniansson et al. *J. Phys. Chem.* **1976**, *80*, 905. Hydrophobic molecules frequently exhibit exit rate constants of less than $10^3 s^{-1}$, cf.: Kalyanasundaram, K.; Thomas, J. K. *J. Am. Chem. Soc.* **1977**, *99*, 2052. A detailed analysis of the $C_{14}MV^+$ kinetics will be published.

(23) The rate constant was measured in dilute viologen solutions where ionic strength effects can be neglected: cf. ref 9.

(19) (a) Jones, M. N.; Reed, D. A. *Kolloid-Z.* **1970**, *235*, 1196. (b) Loeb, A. L.; Overbeck, J. Th.; Wiersema, P. H. "The Electrical Double Layer Around a Spherical Colloid Particle"; MIT Press: Cambridge, Mass., 1961. (c) Fernandez, M. S.; Fromherz, P. *J. Phys. Chem.* **1977**, *81*, 1755. (d) Mukerjee, P.; Banerjee, K. *Ibid.* **1964**, *68*, 3567. (e) Stigter, D. *J. Colloid Interface Sci.* **1967**, *23*, 379.

(20) The probability of encounter of $Ru(bpy)_3^{3+}$ and $ZnTMPyP^{5+}$ with the micellar surface is given by the Boltzmann term $\exp(-z\psi_e/kT)$, where z is the charge of the sensitizer cation and e the elementary charge.

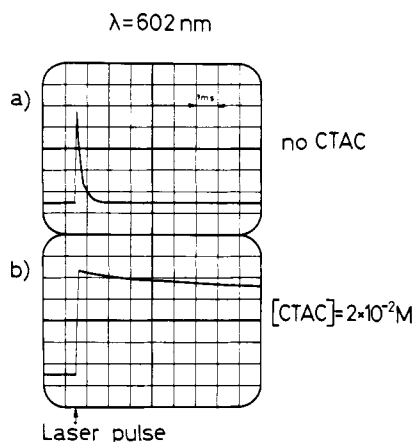


Figure 5. Laser photolysis results illustrating the successful inhibition of the electron back-transfer from $C_{14}MV^+$ to $Ru(bpy)_3^{3+}$ by CTAC micelles: (a) $[Ru(bpy)_3^{2+}] = 10^{-4}$ M; $[C_{14}MV^{2+}] = 5 \times 10^{-4}$ M; (b) added 2×10^{-2} M CTAC.

second-order rate law. Kinetic spectroscopy shows that in the first part of the reaction only the characteristic absorption of the monomer radical is present. However, in the long-time domain a shoulder around 545 nm appears, indicating the presence of multimer forms of the radical. The latter may cause the deviation from a simple second-order rate law observed. In the evaluation of rate constants only the initial part of the decay was considered.

The micellar effects are illustrated in Figure 5 which shows the temporal behavior of the optical density at 602 nm. To clearly demonstrate the charge separation, we selected a relatively long-time scale (10 ms) in the display of the optical events. Both in the absence and presence of CTAC micelles, the signal rises vertically after the laser pulse, indicating the formation of $C_{14}MV^+$. In CTAC-free solution the signal decays steeply thereafter, the return to the base line being completed with 1 ms. In striking contrast to this result stands the behavior observed in the presence of CTAC micelles where there is hardly any decay of the transient over the whole time domain of 10 ms, indicating an astonishingly high stability of the $C_{14}MV^+$ radical. The CTAC system provides a convenient model to check the validity of the kinetic equations elaborated above. Experimentally, one finds⁹ that at CTAC concentrations slightly above the CMC the back-reaction between $C_{14}MV^+$ and $Ru(bpy)_3^{3+}$ occurs in two steps: a fast exponential component followed by a slow part which obeys second-order kinetics. If the CTAC concentration is increased above 5×10^{-3} M, only the slow component remains. Such a behavior is in agreement with the predictions of eq 18. The fast decay arises from the relaxation of the system to quasi-stationary conditions as described by the third term in the equation. As the rate of this process increases exponentially with micellar concentration while its relative contribution to the overall decay decreases,²⁴ then the fast component is only visible at CTAC concentrations close to the CMC ($\sim 1.0 \times 10^{-3}$ M).

The slow decay of the transients should be described by eq 15 which predicts a second-order behavior as indeed is observed. Furthermore, it is expected that the rate constant for the back-reaction decreases with increasing micellar concentration. A test of this prediction is rendered difficult by two facts. First, as was pointed out above, in the disappearance of $C_{14}MV^+$, reactions with O_2 impurities may become rate determining. Second, when the micellar concentrations are varied over a wide range, the electrostatics of the system are changed. At high concentrations overlap of the potential fields of neighboring aggregates occurs reducing the Coulombic repulsion of the oxidized sensitizer from the micellar surface and thus facilitating the back reaction. For this reason, we restricted our investigation to relatively dilute

(24) This contribution is expressed by the term $k_a k_b [M] / (k_a [M] + k_3)$ which decreases with increasing micellar concentration.

Table I. Critical Micelle Concentrations^a of the Surfactant Viologens, C_nMV^{2+} , Employed as Electron Relays

chain length, n	[CMC], M	chain length, n	[CMC], M
12	$(2.0 \pm 0.2) \times 10^{-2}$	16	$(4.2 \pm 1.0) \times 10^{-3}$
14	$(7.5 \pm 0.5) \times 10^{-3}$	18	$(1.4 \pm 0.3) \times 10^{-3}$

^a Obtained for the dibromide salts from the surface tension method.^{4d}

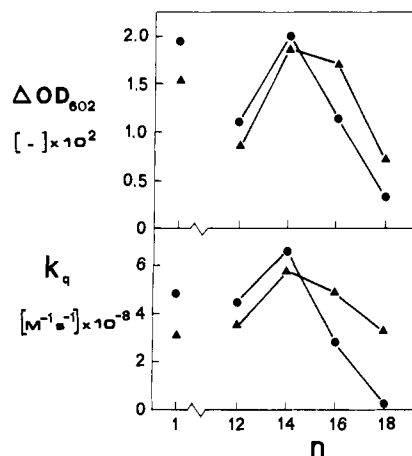


Figure 6. Effect of chain length of the amphiphilic viologen, C_nMV^{2+} , on the yield of redox products as well as the rate constant for quenching of the $Ru(bpy)_3^{2+}$ excited state ($[Ru(bpy)] = 1.36 \times 10^{-4}$ M; $[C_nMV^{2+}] = 7.5 \times 10^{-4}$ M, pure aqueous solution). The data for $n = 1$ refer to simple methyl viologen: (\blacktriangle) no micelles present, (\bullet) 2×10^{-2} M CTAC.

CTAC solutions (5×10^{-3} to 2×10^{-2} M). The trends observed qualitatively confirm the predictions of eq 15 in as much as the rate constant for the back-reaction decreased from 4.0×10^7 to 0.8×10^7 $M^{-1} s^{-1}$ over this concentration range.

The importance of micellar surface charge is also reflected in the results obtained with anionic or nonionic micelles (octaethylene glycol mono-*n*-dodecyl ether). While the former enhance drastically the rate of back-reaction, the latter give only $k_{obsd}/k_b \approx 0.2$ in the case of $C_{14}MV^{2+}$ as electron relay.

(d) Surfactant Viologens with Different Chain Length. In order to optimize the photoproduction and stabilization of reduced viologen, we compared the reactivity of different C_nMV^{2+} derivatives having a chain length between 12 and 18 carbon atoms. Two series of experiments were carried out, one in the absence and the other in the presence of CTAC micelles. In both cases $Ru(bpy)_3^{2+} = 1.36 \times 10^{-4}$ M was used as a sensitizer and the respective C_nMV^{2+} acceptor was present at 7.5×10^{-4} M concentration which for all derivatives is below their CMC value. That the latter condition is fulfilled is apparent from Table I which lists the CMC values of the viologen surfactants employed.

The triangles in Figure 6 depict the effect of chain length on the kinetic parameters k_q as well as the yield of redox products. The latter is expressed in terms of ΔOD_{602} , i.e., the absorbance change at 602 nm after completion of the electron-transfer event. In order to determine the quenching rate constant k_q , we measured the lifetime of the $Ru(bpy)_3^{2+}$ emission in the absence and presence of the respective viologen. Both k_q and ΔOD_{602} augment considerably when the chain length is increased from C_{12} to C_{14} . Further increase in the number of carbons is unfavorable for both the quenching rate as well as the yield of redox products. As far as the rate of the back-reaction is concerned, the trends are less clear. However, all k_b values are well contained within the diffusion-controlled limit, indicating the extremely fast nature of the reverse electron transfer in the absence of micellar aggregates.

As cationic surfactant assemblies are needed to achieve charge separation, it appeared interesting to perform the same series of experiments in the presence of CTAC micelles. These data are indicated as circles in Figure 6. In the case of $C_{12}MV^{2+}$ and $C_{14}MV^{2+}$, ΔOD_{602} as well as k_q increases slightly in the presence

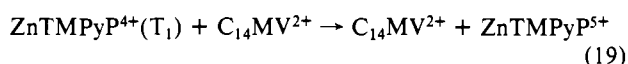
of CTAC micelles. This contrasts with the behavior of $C_{16}MV^{2+}$ and $C_{18}MV^{2+}$ where both parameters are smaller than in CTAC-free solution. The decrease is particularly pronounced for the latter viologen where practically no quenching of the $Ru(bpy)_3^{2+}$ emission and only a very small yield of redox products are observed.

These findings may be rationalized in terms of a partitioning of the C_nMV^{2+} surfactants between the aqueous bulk phase and the micelles. $C_{12}MV^{2+}$ is so hydrophilic that it is only present in water. The kinetic salt effect exerted by monomeric CTAC as well as the volume exclusion of the reactants by the micelles enhance the electron-transfer rate and the yield of redox products. These effects are also dominant in the case of $C_{14}MV^{2+}$ of which only a minor fraction can be associated with the CTAC aggregates. $C_{16}MV^{2+}$ and $C_{18}MV^{2+}$ exhibit a much higher affinity for the micellar phase than the short-chain analogues. The latter seems to be almost completely comicellized with CTAC. As the solubilized viologen cannot be attained by the $Ru(bpy)_3^{2+}$ sensitizer due to electrostatic repulsion of the latter from the micellar surface, no photoreaction is observed.

These data illustrate the necessity of hydrophobic "fine tuning" in the design of a proper electron relay. For the charge separation to succeed, the HLB of the acceptor must be such that the oxidized form is present in the aqueous phase while the reduced form should mainly be associated with the micelles. Both $C_{12}MV^{2+}$ and $C_{14}MV^{2+}$ fulfill this requirement. However, the latter has the advantage over the former in that the photoredox process with $Ru(bpy)_3^{2+}$ is faster and hence produces a higher yield of reduced viologen. We consider it therefore as the optimum choice among the amphiphilic relays investigated here.

(e) Porphyrin-Sensitized Reduction of $C_{14}MV^{2+}$. The principles of light-induced charge separation delineated above should not be restricted to the choice of $Ru(bpy)_3^{2+}$ as a sensitizer. In fact, the utilization of this chromophore in a light energy conversion system is hampered by the relatively short lifetime of its excited state and the 30% upper limit for the quantum yield of viologen reduction. In this respect, the porphyrin $ZnTMPyP^{4+}$ (II) offers distinct advantages over $Ru(bpy)_3^{2+}$. It absorbs further in the visible ($\epsilon_{560} = 1.6 \times 10^4 \text{ M}^{-1} \text{ cm}^{-1}$); the triplet state has a lifetime of 1.3 ms and is produced with ca. 90% efficiency. The triplet has been shown to reduce simple viologen with a high yield²⁵ ($k_q = 2 \times 10^6 \text{ M}^{-1} \text{ s}^{-1}$). Moreover, in the oxidized state this sensitizer has 5 positive charges which should produce a pronounced Coulombic repulsion from the surface of cationic surfactant assemblies.

In the following section we shall be concerned with the reduction of $C_{14}MV^{2+}$ by the triplet state of II.



In particular, the effects of CTAC micelles on the forward and backward electron transfer will be examined. The triplet spectrum of II exhibits a broad band in the 650–1100-nm region.²⁵ The cation $ZnTMPyP^{5+}$, on the other hand, is distinguished by an absorption which rises sharply at wavelengths below 750 nm. The extinction coefficients of the latter at 600 and 700 nm are about equal; in between these two wavelengths there is a shallow minimum. One concludes from these features that the spectrum of $ZnTMPyP^{5+}$ resembles closely that of the simple zinc tetraphenylporphyrin cation.²⁶ In the kinetic analysis we selected $\lambda = 890 \text{ nm}$ for the examination of the triplet decay and $\lambda = 602 \text{ nm}$ for the observation of the redox products.

Data obtained from the laser photolysis of aqueous solutions containing $5 \times 10^{-5} \text{ M}$ $ZnTMPyP^{4+}$ and 10^{-3} M $C_{14}MV^{2+}$ are presented in Figure 7. The upper oscillogram shows the behavior of the 890-nm absorbance. The lifetime of the triplet is about 70 μs which is significantly shorter than in viologen-free solution. From the Stern–Vollmer analysis carried out at relatively small $C_{14}MV^{2+}$ concentrations where the kinetic salt effect plays a negligible role, one obtains $k_q = (1.8 \pm 0.2) \times 10^7 \text{ M}^{-1} \text{ s}^{-1}$. It

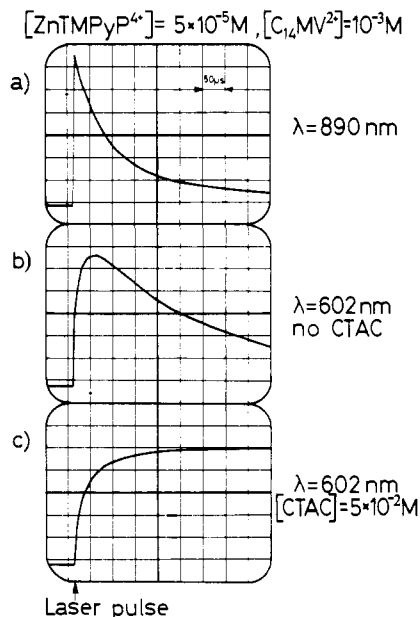


Figure 7. Light-induced reduction of $C_{14}MV^{2+}$ by the triplet state of $ZnTMPyP^{4+}$: (a) triplet decay at 890 nm, (b) growth and decay of redox products in pure aqueous solution, and (c) stabilization of redox products by CTAC micelles.

should be noted that this rate constant is about 10 times higher than the value observed with simple methyl viologen. Apparently, the C_{14} substitution favorably affects the interaction of the redox relay with the porphyrin sensitizer.

Further experiments showed that the quenching process leads to formation of reduced viologen and oxidized porphyrin. This is illustrated in the second oscillogram which displays the time course of the optical density at 602 nm. The signal grows concomitantly with the 890-nm decay. After passing through a maximum, it decays according to a second-order rate law. The kinetic evaluation yields a rate constant of $k_b = 5 \times 10^9 \text{ M}^{-1} \text{ s}^{-1}$, indicating that the back-reaction is diffusion controlled.

A striking change is noted in the dynamics of this redox system when CTAC ($2 \times 10^{-2} \text{ M}$) is added to the solution. In the lowest oscillogram we observe again the rise of the 602-nm absorption which occurs concomitantly with the triplet decay. This time, however, the signal attains a plateau and does not decay at all over a period of 500 μs . Only at time scales as long as 20 ms a decrease in the absorption becomes noticeable. The upper limit for the rate constant of the back-reaction is ca. $10^7 \text{ M}^{-1} \text{ s}^{-1}$, indicating that the electron transfer from $C_{14}MV^{2+}$ to $ZnTMPyP^{5+}$ is blocked efficiently by the CTAC aggregates. The mechanism operative in this system must be similar to the one established for $Ru(bpy)_3^{2+}$: rapid solubilization of the reduced relay in the CTAC micelles which electrostatically reject any approach of the $ZnTMPyP^{5+}$ cation.

A final point concerns the yield of redox products obtained from reaction 19. This was determined by a procedure outlined in detail earlier.^{4a} $Ru(bpy)_3^{2+}$ was dissolved in aqueous 10^{-2} M CTAC until the absorption at 530 nm corresponded exactly to that of a $5 \times 10^{-6} \text{ M}$ $ZnTMPyP^{4+}$ solution in the same medium. The laser dose was then adjusted to a level where $5 \times 10^{-6} \text{ M}$ excited states were produced. This was measured from the absorbance change at 370 nm¹⁷ obtained in the $Ru(bpy)_3^{2+}$ solution immediately after the pulse. The same concentration of excited states was then generated in the porphyrin solution to which 10^{-3} M $C_{14}MV^{2+}$ was added. From the plateau value of the transient optical density at 602 nm the concentration of redox products formed via reaction 19 can be derived. After correcting for the fraction of triplets which are not quenched by $C_{14}MV^{2+}$, one obtains $\eta_{re} = 1.0 \pm 0.1$, indicating practically unit efficiency for the electron transfer.

Apart from the high yield of redox products, i.e., the virtual absence of any cage recombination, reaction 19 is also distin-

(25) Kalayanasundaram, K.; Grätzel, M. *Helv. Chim. Acta* **1980**, *63*, 478.

(26) Fuhrhop, J. H.; Mauzerall, D. *J. Am. Chem. Soc.* **1969**, *91*, 4174.

guished by a surprisingly high efficiency for the conversion of light into chemical energy. As the triplet energy of the porphyrin is about 1.8 eV, one derives from the redox potentials of the two couples $E^\circ(\text{ZnTMPyP}^{5+/4+}) = 1.2 \text{ V}^5$ and $E^\circ(\text{C}_n\text{MV}^{2+/+}) = -0.45 \text{ V}^6$ that more than 90% of the excitation energy is converted into the chemical potential of the redox products.

Conclusion

In the present study pathways were established to prevent the back-reaction of important photoredox reactions by micellar assemblies. Other types of aggregates such as vesicles and surfactant polymers are now under investigations with which the same type of inhibition is conceivable. Crucial with respect to an eventual application of these systems in light energy conversion devices is

the successful coupling of the photoredox reaction with a fuel-producing step which is likely to be catalytic. Particularly encouraging in this regard is the high stability ($\tau > 10 \text{ ms}$) of the intermediates achieved with our systems. The lifetimes obtained are long enough to allow for the intervention of efficient catalysts. Thus, by employing ultrafine Pt particles, we have been able to couple three relays, $\text{C}_{12}\text{Mv}^{2+}-\text{C}_{16}\text{Mv}^{2+}$, with light-induced hydrogen production from water. This subject will be treated in a forthcoming paper.

Acknowledgment. We are grateful for support of this work by the Swiss National Foundation (Grant 2.168.0.78), Ciba-Geigy, Basel (Switzerland) and Engelhard Industries, Metro Park, N.J. (U.S.A.).

Laser Excitation and Emission Spectra of the Hexafluorobenzene Cation in the Gas Phase

Trevor Sears, Terry A. Miller,* and V. E. Bondybey

Contribution from Bell Laboratories, Murray Hill, New Jersey 07974. Received May 5, 1980

Abstract: Laser-induced fluorescence spectra of C_6F_6^+ have been recorded in the gas phase. Excitation spectra of quality far superior to previous observations have been obtained by cooling the ions to near liquid N_2 temperature. The improved S/N and resolution permit considerably more information to be obtained about both the ground $\tilde{X}^2\text{E}_{1g}$ and excited $\tilde{B}^2\text{A}_{2u}$ electronic states. Laser-excited, wavelength-resolved emission spectra have also been observed for C_6F_6^+ . These spectra allow direct observation of the Jahn-Teller perturbed vibronic structure of the ground state. Because of their relative simplicity, assignment and interpretation are usually unambiguous. Overall, the experimental results determine rather extensively and redundantly the vibronic structure of both electronic states.

1. Introduction

The ground electronic state of a molecular cation is usually formed by the removal of one electron from the highest occupied molecular orbital of the parent neutral molecule. For benzene or any of its completely substituted derivatives, e.g., perdeuterio or perfluoro, the relevant orbital is of e_{1g} symmetry and therefore doubly degenerate. The resulting ionic state is consequently $^2\text{E}_{1g}$ and as Jahn and Teller showed¹ is subject to a distortion caused by an interaction between the electronic motion and the vibrational motion corresponding to the normal coordinates of species e_{2g} . As is well-known theoretically, Jahn-Teller distortions cause the minimum of the vibronic potential to be at other than the symmetrical D_{6h} configuration with a concurrent stabilization of the molecular bonding (lowering of the well depth).

Many theoretical papers have been written on Jahn-Teller effects and many experiments, e.g., EPR, photoelectron, visible spectroscopy, have encountered the effect. However it has proven to be nearly impossible to quantitatively measure the Jahn-Teller effect due to various experimental difficulties, averaging effects, lowered site symmetry, spectral resolution, etc. The free, gas-phase, benenoid cations represent a singularly simple and well-characterized opportunity to accomplish the elusive goal of a quantitative, experimental description of the Jahn-Teller effect.

There are obvious attractions in the study of the benzene ion itself, but the spectroscopy of this species is hampered by its extremely low fluorescence quantum yield. However, in 1971, Daintith et al.² reported the emission spectra of the hexafluorobenzene radical cation and Allan and Maier later demonstrated³

that the fluorescence in a series of fluorobenzene cations exhibits a lifetime of around 50 ns and probably occurs with near unity quantum efficiency. A Jahn-Teller distortion is predicted in the ground electronic states of the symmetrically trisubstituted benzene ions (D_{3h}) as well as in the fully fluorinated C_6F_6^+ , and the former have been studied extensively by conventional electronic emission spectroscopy^{4,5} and by a variety of laser-induced fluorescence techniques in both the low-temperature matrix⁶ and gas phases.^{7,8}

The hexafluorobenzene cation emission spectrum as first reported²⁻⁴ is rather broad and unresolved, and its interpretation in terms of ground-state vibronic structure difficult. The same comments apply to the laser-induced fluorescence excitation spectrum in the gas phase⁷ (this experiment yields more information on the vibrational structure in the upper $\tilde{B}^2\text{A}_{2u}$ electronic state involved in the transition which is not degenerate and thus will not show Jahn-Teller type perturbations) which shows extremely dense vibrational structure presumably due to sequence band congestion. The spectra taken in a low-temperature matrix environment do not suffer from this complication, and both the laser excitation and emission spectra have been recently reported in detail.⁹ The spectra taken in a Ne matrix offer considerable insight into the vibrational structure of the ground state.

Information obtainable from gas-phase spectra is still desirable from several points of view. First, even though there is now considerable evidence concerning the lack of perturbation in the Ne matrix, any direct corroboration of the matrix data is always

(4) C. Cossart Magos, D. Cossart, and S. Leach, *J. Chem. Phys.*, **69**, 4313 (1978); *Mol. Phys.*, **37**, 973 (1979).

(5) C. Cossart Magos, D. Cossart, and S. Leach, *Chem. Phys.*, **41**, 345 (1979); *Chem. Phys.*, **41**, 363 (1979).

(6) V. E. Bondybey, T. A. Miller, and J. H. English, *J. Chem. Phys.*, **71**, 1088 (1979).

(7) V. E. Bondybey and T. A. Miller, *J. Chem. Phys.*, **70**, 138 (1979).

(8) T. A. Miller, V. E. Bondybey, and J. H. English, *J. Chem. Phys.*, **70**, 2919 (1979).

(9) V. E. Bondybey and T. A. Miller, *J. Chem. Phys.*, **73**, 3053 (1980).

(1) H. A. Jahn and E. Teller, *Proc. R. Soc. London., Series A* **161**, 220 (1900).

(2) J. Daintith, R. Dinsdale, J. P. Maier, D. A. Sweigart, and D. W. Turner, "Molecular Spectroscopy", Institute of Petroleum: London, 1971, p 16.

(3) M. Allan and J. P. Maier, *Chem. Phys. Lett.*, **34**, 442 (1975); M. Allan, J. P. Maier, and O. Marthaler, *Chem. Phys.*, **26**, 131 (1977).